The Astronomical Journal, 158:53 (8pp), 2019 August https://doi.org/10.3847/1538-3881/ab27bc

Colors of Trans-Neptunian Contact Binaries

Audrey Thirouin[1] and Scott S. Sheppard[2]
[1] Lowell Observatory, 1400 W. Mars Hill Road, Flagstaff, AZ 86001, USA; thirouin@lowell.edu
[2] Department of Terrestrial Magnetism (DTM), Carnegie Institution for Science, 5241 Broad Branch Road NW, Washington, DC, 20015, USA
Received 2019 April 22; revised 2019 June 3; accepted 2019 June 5; published 2019 July 10

Abstract

The $g'r'i'$ colors of seven likely and potential contact binaries in the Kuiper Belt were acquired with the *Magellan-Baade* telescope and combined with colors from the literature to understand contact binary surfaces. The likely and potential contact binaries discovered in the dynamically cold classical population display very red/ultra-red colors. Such colors are common in this sub-population and imply that the cold classical contact binaries were formed in situ. The likely contact binaries found in several mean motion resonances with Neptune have colors from moderately to ultra-red, suggesting different formation regions. Among the nine contact binaries discovered in resonances, five have very red/ultra-red colors and four have moderately red surfaces. Based on the very red/ultra-red colors and low to moderate inclinations of the contact binaries in resonances, these contact binaries are possibly escaped dynamically cold classicals that are now trapped in resonances. Moderately red surfaces are common in diverse sub-populations of the Kuiper Belt, thus pinpointing their origin is difficult though they are most likely captured objects that formed in the giant planet area. Finally, for the contact binary population we report an anti-correlation between inclination and g'–r', as noticed in the rest of this belt. We also find hints of trends between eccentricity, perihelion distance, rotational period, and g'–r', but as we are still dealing with a limited sample, additional data are required to confirm them.

Key words: Kuiper belt objects: individual (2004 VC_{131}, 2004 VU_{75}, 2012 DX_{98}, 2013 FR_{28}, 2014 JL_{80}, 2014 JO_{80})

1. Contact Binaries

Contact and close binaries are found in abundance across the solar system in most of the small-body populations (Mann et al. 2007; Benner et al. 2015; Massironi et al. 2015; Agarwal et al. 2017; Ryan et al. 2017). In the Kuiper Belt, the existence of tight binaries was suspected but undiscovered, as they are below the resolution of the *Hubble Space Telescope* (*HST*; Porter & Grundy 2012). Nevertheless, Sheppard & Jewitt (2004) found that the light curve of 2001 QG_{298} was compatible with a contact binary configuration. They also estimated that the percentage of contact binaries should be ∼30%. Because of a significant change in amplitude for the light curve of 2001 QG_{298}, Lacerda (2011) modeled the system and concluded that if contact binaries have a similar large obliquity, we underestimated their fraction.

Recently, several likely and potential contact binaries were found in the Kuiper region through light-curve studies (Lacerda et al. 2014; Thirouin et al. 2017; Thirouin & Sheppard 2017, 2018, 2019; Rabinowitz et al. 2018, D. L. Rabinowitz et al. 2019, in preparation). The definition of likely, confirmed, and potential contact binaries is available in Thirouin & Sheppard (2019). To summarize, confirmed contact binaries display a light-curve amplitudes larger than 0.9 mag and a U-/V-shape morphology, whereas a likely contact binary also has large amplitude, but below the 0.9 mag threshold. Also, in Thirouin & Sheppard (2019) we reported several potential contact binaries showing a large light-curve amplitude, but unfortunately we lacked a full light-curve that would allow us to classify them as likely/confirmed contact binaries, and thus to be conservative we considered them potential contact binaries, as more data are needed to classify them. Finally, the flyby of 2014 MU_{69} by the *NASA New Horizons* spacecraft and its stellar occultation confirmed that this dynamically cold classical trans-Neptunian object (TNO) is also a contact binary (Moore et al. 2018; Stern et al. 2019). Currently, the census of contact binaries is:

1. In the dynamically cold classical population: one confirmed, 2014 MU_{69}, two likely, 2002 CC_{249} and 2004 VC_{131}, and two potential, 2004 MU_8 and 2004 VU_{75} (Thirouin & Sheppard 2017, 2019).
2. In the 3:2 resonance (or Plutino population): one confirmed, 2001 QG_{298}, and four likely, 2014 JQ_{80}, 2014 JO_{80}, 2014 JL_{80} and 2000 GN_{121} (Sheppard & Jewitt 2004; Lacerda 2011; Thirouin & Sheppard 2018).
3. In the 2:1 resonance (or twotino): one likely, 2012 DX_{98} (A. Thirouin & S. S. Sheppard 2019, in preparation).
4. In the 7:4 resonance: Manwë–Thorondor is a resolved wide binary and to interpret the mutual event season, it has been argued that Manwë (i.e., the primary) is a contact binary (Rabinowitz et al. 2017, 2018). 2013 FR_{28} is also a likely contact binary based on its large-amplitude partial light curve (A. Thirouin & S. S. Sheppard 2019, in preparation).
5. In the 5:2 resonance: one likely, 2004 TT_{357} (Thirouin et al. 2017).
6. In the Haumea family: one likely, 2003 SQ_{317} (Lacerda et al. 2014).

To summarize, the contact binary population can be up to 15 TNOs: 5 dynamically cold classical , 9 resonant TNOs, and 1 in the Haumea family. Based on the number of objects observed for large-amplitude light curves, Thirouin & Sheppard (2018) found that 40%–50% of the Plutinos are equal-sized contact binaries, while Thirouin & Sheppard (2019) found only 10%–25% of cold classicals are likely nearly equal-sized contact binaries. This suggests that dynamical evolution is important in contact binary formation.

So far, we have studied the contact binary rotational properties but in this work, we will focus on their surface

Table 1
Observing Circumstances

TNO	UT-date [YYYY/MM/DD]	r_h (au)	Δ (au)	α (deg)	Dyn. Class.	i (deg)	g'–r' (mag)	g'–i' (mag)	Reference
2004 VC_{131}	2018 Dec 12	40.776	39.852	0.5	Cold	0.5	0.89 ± 0.06	1.40 ± 0.05	This work
2004 VU_{75}	2018 Dec 12	43.667	42.933	0.9	Cold	3.3	0.96 ± 0.06	1.42 ± 0.05	This work
2012 DX_{98}	2019 Mar 1	34.376	35.123	1.1	2:1	13.1	0.85 ± 0.06	1.25 ± 0.06	This work
2013 FR_{28}	2019 Mar 2	33.577	34.253	1.2	7:4	3.0	0.95 ± 0.05	1.36 ± 0.05	This work
2014 JL_{80}	2019 Feb 3	28.471	28.749	1.9	3:2	6.2	0.74 ± 0.05	⋯	This work
2014 JO_{80}	2018 May 17	32.192	31.231	0.6	3:2	15.7	0.67 ± 0.03	0.91 ± 0.03	This work
2014 JQ_{80}	2019 Mar 3	31.686	31.850	1.8	3:2	8.0	0.76 ± 0.05	1.05 ± 0.05	This work
2004 TT_{357}	⋯	⋯	⋯	⋯	5:2	9.0	0.74 ± 0.03	0.99 ± 0.04	Thirouin et al. (2017)
(139775) 2001 QG_{298}[a]	⋯	⋯	⋯	⋯	3:2	6.5	0.80 ± 0.03	⋯	Sheppard & Jewitt (2004)
(47932) 2000 GN_{171}[a]	⋯	⋯	⋯	⋯	3:2	10.8	0.80 ± 0.04	1.21 ± 0.04	Sheppard & Jewitt (2002)
(385446) 2003 QW_{111}	⋯	⋯	⋯	⋯	7:4	2.7	0.85 ± 0.06	1.20 ± 0.05	Sheppard (2012)
(126719) 2002 CC_{249}	⋯	⋯	⋯	⋯	Cold	0.8	0.97 ± 0.06	1.24 ± 0.05	Thirouin & Sheppard (2017)
(486958) 2014 MU_{69}[a]	⋯	⋯	⋯	⋯	Cold	2.5	0.95 ± 0.14	1.42 ± 0.14	Benecchi et al. (2018)
2004 MU_8	⋯	⋯	-	⋯	Cold	3.6	1.15 ± 0.17	⋯	Petit et al. (2011)
2003 SQ_{317}[a]	⋯	⋯	⋯	⋯	Haumea	28.6	0.46 ± 0.18	⋯	Lacerda et al. (2014)

Notes. All runs made use of the Sloan filters ($g'r'i'$). Two columns are for the objects' dynamical classification and inclination. The last seven objects have colors that are already published (i.e., no observing log to report). The case of Manwë–Thorondor ((385446) 2003 QW_{111}) will be discussed in Section 4.
[a] Objects with colors in the BVRI filters that Smith et al. (2002) used to convert to the Sloan filter system.

colors. The Kuiper Belt has a variety of colors, from neutral to ultra-red objects (Doressoundiram et al. 2008; Peixinho et al. 2015; Marsset et al. 2019). Some sub-populations are showing some specific color characteristics. The dynamically cold classical population has mostly only very red/ultra-red colors (Peixinho et al. 2004). The resonances 7:4 and 5:3 within the main Kuiper Belt are mostly ultra-red. The 3:2 and 2:1 resonances, just interior and exterior of the Kuiper Belt are a mixture of colors. The 5:2, 3:1, and more distant resonances show mostly only moderately red colors (Sheppard 2012). The very red/ultra-red colors indicate an in situ formation beyond Neptune, whereas the mixture of colors suggest that objects formed in the inner and outer solar system are now trapped in some resonances (Fraser & Brown 2012; Sheppard 2012).

In this paper we report new colors for seven contact binaries and summarize the already published colors of seven more. We will use colors to pinpoint where these contact binaries may have formed, and we will look for tendencies between colors and orbital elements that may differentiate the contact binaries from other TNOs.

2. Observations and Reduction

Data were obtained with the *Magellan-Baade* telescope at Las Campanas Observatory (Table 1). For all the observing runs, the wide-field imager named IMACS was used. IMACS has eight 2k × 4k CCDs and a field of view of 27.′4.

When observing an object for colors, it is crucial to take into account its light curve (Schwamb et al. 2018). In fact, the light-curve amplitude correction will affect the colors of moderate-to large-variability objects. To minimize such an effect, images were taken consecutively, thus the amplitude correction is not needed. Rotational periods of the objects in this work are between 6 and 35 hr (some periods are still to be determined, but seem to be longer than 10 hr). Our exposure times were between 300 and 500 s depending on filters and the brightness of the objects, thus we are only covering a small fraction of the full rotation during the color measurements.

Every night, several biases and dome flats (in the g', r', and i' filters) were taken to create a median flat (in each filter) and a median bias to correct the science images. Standard fields from Smith et al. (2005) were also imaged for absolute calibration purposes. Finally, the growth curve technique was used to select the optimal aperture radius (Howell 1989). Our procedure is detailed in Thirouin et al. (2012).

3. Color Results: New and Published

As displayed in Figure 1, we first report new colors of seven likely and potential contact binaries discovered by Thirouin & Sheppard (2018, 2019). Second, we summarize the already published colors of five likely/confirmed contact binaries. In this section, we will focus on contact binaries identified through light-curve studies. The special cases of 2014 MU_{69} and Manwë–Thorondor will be discussed in the next section.

3.1. New cold classical Contact Binary Colors

2004 VC_{131}. This dynamically cold classical rotates every 15.7 hr and has a variability of 0.55 mag (Thirouin & Sheppard 2019). Its colors are ultra-red and are typical of the cold classical population: g'–$r' = 0.89 \pm 0.06$ mag and g'–$i' = 1.40 \pm 0.05$ mag.

3.2. New Resonant Contact Binary Colors

2014 JL_{80}. With a periodicity of about 35 hr, the Plutino 2014 JL_{80} is the slowest likely contact binary reported so far (Thirouin & Sheppard 2018). We imaged 2014 JL_{80} and computed g'–$r' = 0.74 \pm 0.05$ mag. This color suggests a moderately red surface.

2014 JO_{80}. Thirouin & Sheppard (2018) identified 2014 JO_{80} as a likely Plutino contact binary. Based on data obtained on 2018 May 17th, we derive moderately red colors: g'–$r' = 0.67 \pm 0.03$ mag, r'–$i' = 0.24 \pm 0.03$ mag. and g'–$i' = 0.91 \pm 0.03$ mag.

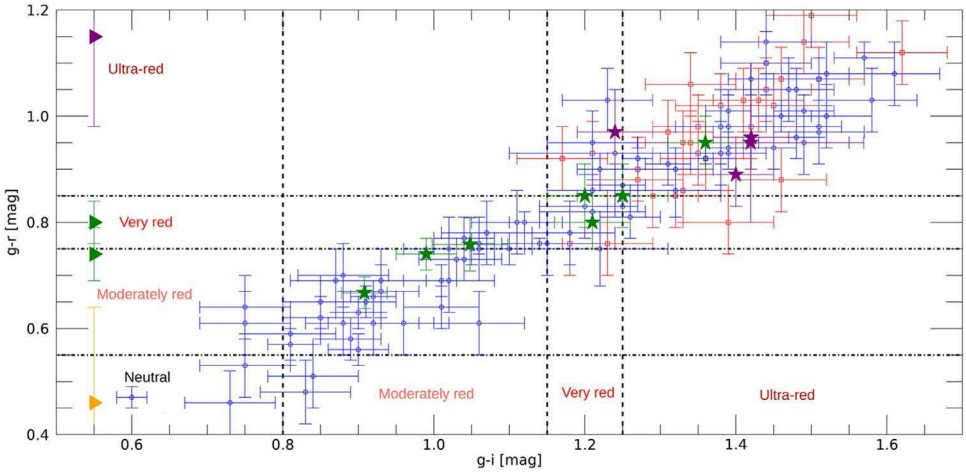

Figure 1. Colors of resonant (blue open circles) and dynamically cold classical TNOs (red open squares) are plotted for non-contact binaries. Values are from Sheppard (2012), Peixinho et al. (2015), and references therein. Dynamically cold classicals discussed in this work as potential/likely contact binaries are indicated with a purple star, whereas the resonant potential/likely contact binaries are plotted with a green star. As the *i* bands for 2001 QG_{298}, 2003 SQ_{317}, 2004 MU_8, and 2014 JL_{80} are not available, only the g'–r' are plotted (green right triangles for resonant objects, orange for the Haumea family member, and a purple triangle for the cold classical). In the case of 2004 MU_8, there is one image in the i' band but for reasons detailed in Section 3, we are not considering it. Manwë–Thorondor and 2014 MU_{69} are included in this plot.

2014 JQ_{80}. Thirouin & Sheppard (2018) reported 2014 JQ_{80} as a likely contact binary in the Plutino population. Based on images obtained in 2019 March, we estimate moderately red colors: g'–$r' = 0.76 \pm 0.05$ mag and g'–$i' = 1.05 \pm 0.05$ mag.

2012 DX_{98}. This 2:1 resonant object has a periodicity of 20.80 h, a variability of 0.47 mag, and its light-curve morphology suggests a contact binary configuration (A. Thirouin & S. S. Sheppard 2019, in preparation). Its colors are very red: g'–$r' = 0.85 \pm 0.06$ mag and g'–$i' = 1.25 \pm 0.06$ mag.

2013 FR_{28}. This resonant 7:4 object is a likely contact binary based on its variability of about 0.8 mag in a few hours (A. Thirouin & S. S. Sheppard 2019, in preparation). Based on data carried out in 2019 March, we find an ultra-red color: g'–$r' = 0.95 \pm 0.05$ mag and g'–$i' = 1.36 \pm 0.05$ mag.

3.3. New and Published Target of Interest Colors

The next two objects, 2004 MU_8 and 2004 VU_{75}, were identified as targets of interest based on their large light-curve amplitudes over a few hours (Thirouin & Sheppard 2019).

2004 MU_8. Petit et al. (2011) reported some color information for 2004 MU_8. More details are available regarding these colors at the Besançon photometric database for Kuiper Belt Objects and Centaurs.[3] There are four g' bands, four r' bands and one i' band. Unfortunately, the data are from several nights and the g' and r' bands are not consecutive, so light-curve amplitude can be an issue. The median in g′ is 6.82 mag and the median in r′ is 5.66 mag, so g'–$r' = 1.15$ mag, suggesting that 2004 MU_8 is ultra-red. But further observations should be obtained to confirm this color.

2004 VU_{75}. This target of interest displays a variability of ∼0.4 mag over a few hours. Thirouin & Sheppard (2019) presented several potential light curves but did not favor any option. The colors of 2004 VU_{75} are: g'–$r' = 0.96 \pm 0.06$ mag and g'–$i' = 1.42 \pm 0.05$ mag. This ultra-red color is typical of the cold classical population.

[3] https://bdp-obs.utinam.cnrs.fr/src_base/download.php

3.4. Published Contact Binary Colors

Several confirmed/likely contact binaries have color results already published.

2002 CC_{249}. This dynamically cold classical TNO was identified as a likely contact binary by Thirouin & Sheppard (2017). They found an ultra-red color of g'–$r' = 0.97 \pm 0.06$ mag and g'–$i' = 1.24 \pm 0.05$ mag.

2001 QG_{298}. Sheppard & Jewitt (2004) classified this Plutino as a contact binary based on its light-curve morphology and the extreme amplitude of 1.14 mag. Lacerda (2011) obtained a second light curve with a smaller amplitude of 0.7 mag. The amplitude change is compatible with a system with a large obliquity observed at different viewing geometries. Sheppard & Jewitt (2004) estimated the following colors[4]: V–$R = 0.60 \pm 0.02$ mag and B–$V = 1.00 \pm 0.04$ mag. There is no *I*-band available for this object.

2000 GN_{171}. Sheppard & Jewitt (2002) reported the first light curve of the Plutino 2000 GN_{171} with a rotation of 8.3 h for a variability of 0.61 mag. The second light curve obtained by Dotto et al. (2008) confirmed such a find. Lacerda & Jewitt (2007) inferred that the light curve can be due to a triaxial ellipsoid or due to a contact binary. Recently, we favored the contact binary option (see Thirouin & Sheppard 2018 for details). Colors[5] obtained by several teams are in agreement: V–$R = 0.63 \pm 0.03$ mag, B–$V = 0.92 \pm 0.04$ mag, and R–$I = 0.56 \pm 0.03$ mag (Boehnhardt et al. 2002; Sheppard & Jewitt 2002; Doressoundiram et al. 2007; Tegler et al. 2016).

2004 TT_{357}. Sheppard (2012) collected a large color data set for objects in Neptune's resonances. 2004 TT_{357} was one of the 5:2 resonant in this sample. Sheppard (2012) calculated the following colors: g'–$r' = 0.74 \pm 0.03$ mag and g'–$i' = 0.99 \pm 0.04$ mag.

2003 SQ_{317}. Lacerda et al. (2014) obtained a large-amplitude light curve (0.85 mag) with a period of 7.21 hr for this object. They also measured a B–$R = 1.05 \pm 0.18$ mag. 2003 SQ_{317}

[4] The conversion to the Sloan system gives g'–$r' = 0.80 \pm 0.03$ mag.

[5] We calculated g'–$r' = 0.80 \pm 0.04$ mag and g'–$i' = 1.21 \pm 0.04$ mag (Smith et al. 2002).

belongs to the Haumea family[6] (Snodgrass et al. 2010; Lacerda et al. 2014).

4. Discussion

4.1. The Dynamically cold classical Population

So far, two likely contact binaries (2004 VC_{131} and 2002 CC_{249}) and two potential contact binaries (2004 MU_8 and 2004 VU_{75}) have been identified in the dynamically cold classical population through light-curve studies (Thirouin & Sheppard 2017, 2019). To this list, we have to add 2014 MU_{69}, which, based on the *New Horizons* flyby, is a contact binary (Stern et al. 2019). Colors of 2014 MU_{69} were obtained before the flyby with the *HST*. Benecchi et al. (2018) reported a very red surface for this object with a F606W–F814W = 1.03 ± 0.14 mag[7] using the *HST* set of filters. Using Benecchi et al. (2018) and Smith et al. (2002), we derived g'–i' = 1.42 ± 0.14 mag and g'–r' = 0.95 ± 0.14 mag for 2014 MU_{69}. This very red color was confirmed by the flyby data (Stern et al. 2019).

In Figure 1, color results for these five contact binaries are plotted. They all[8] have a g'–r' > 0.85 mag, suggesting that their surfaces are ultra-red. This color is typical of the dynamically cold classical TNOs, which may be further distinguished by their color through z-band photometry (Pike et al. 2017). It is thought that the dynamically cold classicals have been formed roughly where they are now, and they never suffered any catastrophic collisional processes (Batygin et al. 2011). With an in situ formation, they are considered the most pristine objects among the TNOs and their surfaces are also likely primordial. As our likely/potential contact binaries and 2014 MU_{69} also display the typical color of the rest of the dynamically cold classical TNOs, they have likely also formed in situ, and thus are not interlopers in this population.

4.2. The 3:2, 2:1, 7:4, and 5:2 Resonances

Neptune's mean motion resonances are interesting for understanding Neptune's migration toward the outer solar system as well as constraining whether the migration was smooth or grainy (Nesvorný 2015). Sheppard (2012) studied in detailed the color distribution of resonant TNOs using new data and the literature. Thirteen resonances were studied in Sheppard (2012), but here we will only discuss the resonances where contact binaries have been discovered (i.e., 3:2, 2:1, 7:4, and 5:2). The dynamically cold classical population is "delimited" by the 3:2 (at 39.4 au) and 2:1 resonances (47.8 au). The 3:2 and 2:1 resonances have a large variety of colors, suggesting that these resonances have trapped objects from different areas of the solar system. The distant 5:2 resonance at 55.4 au is dominated by moderately red objects, unlike the 7:4 (at 43.7 au) within the main classical Kuiper Belt that has only ultra-red objects (Sheppard 2012).

So far, only one TNO in the 5:2 resonance is classified as a likely contact binary, 2004 TT_{357} with moderately red color, similar to the color found for most 5:2 objects.

In the 2:1, 2012 DX_{98} is a likely contact binary with a very red surface. In the 3:2 resonance, five likely/confirmed contact binaries have been found: 2001 QG_{298} and 2000 GN_{171} with very red surfaces, and 2014 JL80, 2014 JQ_{80}, and 2014 JO_{80} with a moderately red surface; thus the 3:2 contact binaries show a range of colors, like the general 3:2 population.

In the 7:4, 2013 FR_{28} displays an ultra-red color. Lots of ultra-red TNOs have been found at low inclination in the 5:3 and 7:4 resonances. Such a find is not surprising, as these resonances are near the dynamically cold classical population, at 42.3 and 43.7 au. These ultra-red objects were likely formed in the cold classical population but are now trapped in resonances (i.e., escaped cold classicals).

Based on their color survey, Sheppard (2012) also found low-inclination ultra-red objects in inner and outer resonances, suggesting that escaped cold classicals can be trapped further out and in from their main reservoir between the 3:2 and 2:1 resonances. Once trapped in resonances, objects can dynamically diffuse and end up with higher inclination. Therefore, finding escaped cold classicals at higher inclinations is possible.

The 2:1 object, 2012 DX_{98}, could be an escaped cold classical based on its very red color. 2013 FR_{28} is likely from the cold classical population based on its ultra-red color. The very red colors of the Plutinos 2000 GN_{171} and 2001 QG_{298} make them possible candidates that escaped the cold classical region.

Four of our likely contact binaries, 2014 JL_{80}, 2014 JO_{80}, 2014 JQ_{80}, and 2004 TT_{357}, have moderately red surfaces and thus are not linked to the dynamically cold classical population. Moderate colors are typical of the scattered disk, the detached objects, and the hot classicals, and thus we are not able to pinpoint the exact origin of these three likely contact binaries (Sheppard 2012).

Finally, we highlight the case of Manwë–Thorondor (also known as (385446) 2003 QW_{111}). This object is a resolved wide binary in the 7:4 resonance at low inclination (Grundy et al. 2014). In order to interpret the light curve of this system, as well as its mutual event season, it is proposed that the primary, Manwë, is a contact binary (Rabinowitz et al. 2018, D. L. Rabinowitz et al. 2019, in preparation). The colors of the system have been obtained by Sheppard (2012) as g'–r' = 0.85 ± 0.06 mag, g'–i' = 1.20 ± 0.05 mag, and r'–i' = 0.40 ± 0.04 mag. These values are consistent with Grundy et al. (2014) estimates using *HST* data. Therefore, Manwë–Thorondor displays a very red surface close to the ultra-red region, thus it is likely from the cold classical population.

4.3. The Haumea Family

The Haumea family was discovered as a cluster of objects with similar icy surface compositions and proper orbital elements by Brown et al. (2007). Over the years, several objects have been added to the family and it has also been argued that rockier members could be part of the family too (Brown et al. 2007; Ragozzine & Brown 2007; Schaller & Brown 2008; Snodgrass et al. 2010; Trujillo et al. 2011; Volk & Malhotra 2012). Light curves have been analyzed for the members and candidates of the family (Carry et al. 2012; Lacerda et al. 2014; Hastings et al. 2016; Thirouin et al. 2016). One of the confirmed members, 2003 SQ_{317} is a likely contact binary and was characterized by Lacerda et al. (2014). This object has the typical neutral to blue color of the rest of the icy family members. It is unclear how this object formed, mainly because it it still unclear how the family formed. Rotational fission, graze and merge impacts, and catastrophic collision

[6] g'–r' = 0.46 ± 0.18 mag using the previously mentioned conversion.

[7] Benecchi et al. (2018) converted this set of filters to V–I = 1.35 mag.

[8] 2014 MU_{69} is close to our very red/ultra-red separation, but we want to emphasize that we had to convert the Benecchi et al. (2018) color estimate to g'–r' and thus the uncertainty is larger than wanted.

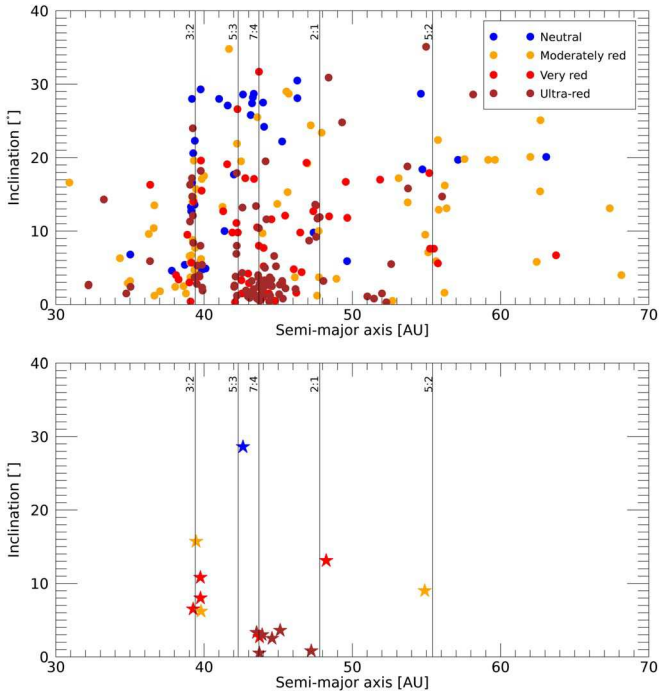

Figure 2. Color distribution in the Kuiper Belt. We plotted all TNOs with known colors (upper plot). Only objects with a semimajor axis from 30 to 70 au are reported for clarity. The stars in the lower plot represent the contact binaries reported in this work. The same color coding is used for both plots.

have been proposed but none of these models are able to fully match the observables (Brown et al. 2007; Schlichting & Sari 2009; Leinhardt et al. 2010; Ortiz et al. 2012; Campo Bagatin et al. 2016). As the history of this family is different than the rest of the TNOs, this family should be treated as a separate case. The formation of 2003 SQ_{317} as a contact binary is likely different from the formation of the other contact binaries.

4.4. Colors versus Orbital Elements, Sizes, and Rotational Periods

First, we emphasize that the number of contact binaries in the Kuiper Belt is still very limited, thus all the trends presented in this subsection have to be taken with caution. It is necessary to discover and characterize more contact binaries to improve our understanding of this population.

As mentioned above, escaped cold classical TNOs have been found in several resonances, generally at low inclination, but some are also at higher inclinations (Sheppard 2012). The very red/ultra-red resonant contact binaries have inclinations from $i = 2\overset{\circ}{.}7$ to $13\overset{\circ}{.}1$, whereas the moderately red resonants have $i = 6\overset{\circ}{.}2$–$15\overset{\circ}{.}7$ (Table 1, Figure 2). In all cases, the resonants discussed in this work have low to moderate inclinations ($2\overset{\circ}{.}7$–$15\overset{\circ}{.}7$). In the case of the cold classicals, their inclinations are lower than $3\overset{\circ}{.}6$, whereas the Haumea family member has the highest inclination, with $i = 28\overset{\circ}{.}6$.

There is an anti-correlation between inclination and g'–r', suggesting that the redder objects are at lower inclination (Figure 3). Using the Spearman (1904) technique, this anti-correlation has a $\rho = -0.740$ and a significance level of 99% using our entire sample. Without the Haumea family member, we have $\rho = -0.680$ and a significance level of 99%.

The anti-correlation between inclination and color was first noticed by Tegler & Romanishin (2000) for the classical population. In fact, the ultra-red material is at low inclination, with a cutoff of 5°–10°, and it corresponds to the dynamically cold classical TNOs. Several studies looked for similar anti-correlation across the sub-populations as well as the entire belt (Trujillo & Brown 2002; Sheppard 2012; Peixinho et al. 2015; Tegler et al. 2016; Marsset et al. 2019). Using the entire belt, the tendency was not obvious but a recent study by Marsset et al. (2019) suggests that such a trend exists. Therefore, the contact binary sample seems to follow the same tendency as the rest of the trans-Neptunian belt.

There is an anti-correlation between eccentricity and g'–r', suggesting that the redder objects are at low eccentricity, but the significance level is low. Using the entire sample, we found $\rho = -0.505$ with a significance level of 94%, Without the Haumea family member (2003 SQ_{317}), we estimated $\rho = -0.706$ at 99%. Also, there is a potential correlation between colors and perihelion distance. With the entire sample, the correlation has a $\rho = 0.593$ for a significance level of 97%, but without 2003 SQ_{317} we found $\rho = 0.815$ at 99%. There is no evidence for strong correlation/anti-correlation between colors and perihelion distance and eccentricity among the entire trans-Neptunian belt (Peixinho et al. 2015). Therefore, it is unclear if these trends are characteristic of the contact binary population or if we are dealing with an observational bias due to our limited sample.

Rotational periods have been derived for most of the confirmed and likely contact binaries. Only 2004 VU_{75}, 2004 MU_8, and 2013 FR_{28} do not yet have a rotational light curve. We found a potential correlation between colors and periods, suggesting that the redder objects are slow rotators. Using our entire sample, we computed $\rho = 0.471$ at 88% but without 2014 JL_{80} (the slowest rotator), $\rho = 0.680$ at 97% (Figure 3). Color indicates age: bluer objects have younger surfaces and redder objects are primordial older surfaces. Collisions can expose icy material and thus resurface an object and make it bluer, as well as affect its rotation. Assuming that collisions spin up the rotation, the bluer objects are the youngest, they are fast rotators, and they have suffered strong collisional history. However, Thirouin et al. (2016) inferred that the Haumea family members (i.e., blue objects) tend to rotate faster than the other TNOs and Thirouin & Sheppard (2019) suggested that the dynamically cold classical TNOs (i.e., very red/ultra-red objects) tend to rotate slowly. In both studies, we argued that these differences are likely due to the formation/evolution of these objects. It also seems likely that the escaped cold classicals identified as likely contact binaries are also rotating slower than the rest of the TNOs, like the rest of the dynamically cold classical TNOs (Thirouin & Sheppard 2019).

Finally, we also looked for any trend between colors and absolute magnitude (Figure 3). There is no obvious trend. Similarly, there is no trend between colors and the other orbital elements.

4.5. Implications for the Formation of Contact Binaries

The contact binary population does not display any significant differences in color compared to the rest of the TNOs (based on our limited sample).

In Thirouin & Sheppard (2018, 2019), we found that 40%–50% of the Plutinos and only 10%–25% in the dynamically cold classical population could be nearly equal-sized contact

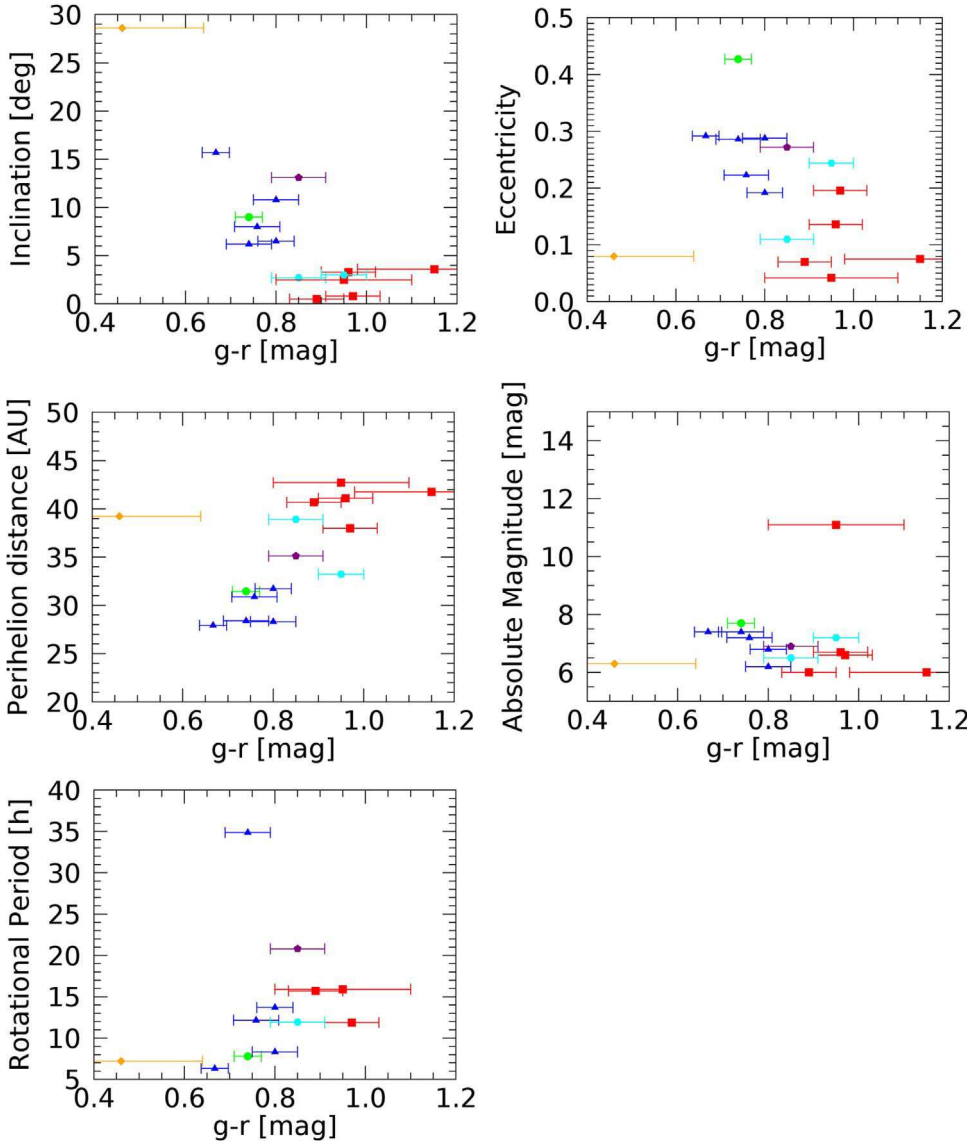

Figure 3. Orbital elements, absolute magnitude, and rotational period vs. g'–r': Objects discussed in this work are plotted. The legend is: red squares for dynamically cold classicals, blue triangles for Plutinos, a green circle for the 5:2 resonant, a cyan hexagon for the 7:4 resonants, a purple hexagon for the 2:1 object and an orange diamond for the Haumea family member. There is an anti-correlation between inclination and g'–r' and a correlation between rotational period and colors.

binaries. There is no estimate for the 2:1, 7:4, and 5:2 resonances yet, but if they are similar to the 3:2 resonance, we can expect a large number of contact binaries. Also, it seems that the resonances are a good place to look for contact binaries, as more than half of them have been found in resonances.

How contact binaries form is still an open question. Four models have been proposed: (i) Kozai and other dynamical effects can shrink the orbit of wider binaries (Porter & Grundy 2012), (ii) fragmentation during gravitational collapse of a cloud of particles during formation (Nesvorný et al. 2010), (iii) three-body type interactions (Goldreich et al. 2002), and (iv) gentle collision between two objects (Stern et al. 2019). Because the dynamically cold classical population never suffered any strong collisional evolution, the gentle collision process seems to be an adequate option, but we cannot discard the other options. However, because different resonances have different formations and evolutions, the gentle collision seems unlikely to explain the creation of contact binaries in resonances. These differences in dynamical history also likely account for the difference in the wide binary fraction seen for the cold classicals compared to the resonances and scattered disk objects (see Thirouin & Sheppard 2019). That is, the more significant dynamical interactions likely experienced by the resonance and scattered objects caused most wide binaries to be unstable, with the wide secondary either being lost from the system or possibly collapsing down to form a closer or contact binary (see also Thirouin & Sheppard 2019 and Nesvorný & Vokrouhlický 2019).

Despite finding a handful of contact binaries in the dynamically cold classicals, we have hints, based on their ultra-red/very red colors and low/moderate inclinations, that several escaped cold classicals are contact binaries. In fact, there are 10 ultra-red/very red (5 in resonances and 5 in the cold classical population) and 5 moderately red/neutral contact binaries. Therefore, despite the limited sample, it seems that some of the contact binaries in resonances are linked (or potentially) to the cold classicals.

For the escaped cold classical contact binaries, it is necessary to discuss where they have been formed. The contact binary could have been formed in the dynamically cold classical population and escaped as a contact binary or it could have been formed once in resonance (or during its escape). As the dynamically cold classical population is dominated by resolved wide binaries it is not unrealistic to expect that resolved wide binaries were able to escape their main reservoir and are now trapped in resonances. With the discovery of a wide binary with ultra-red color in the 3:2 population ((341520) Mors-Somnus, 2007 TY_{430}), the feasibility of this scenario has been demonstrated (Sheppard et al. 2012). Then, through dynamical processes and/or tidal effects, these wide binaries could shrink their orbits and end up as contact binaries. On the other hand, if a wide binary like 2007 TY_{430} is able to conserve its binarity after escaping the dynamically cold classical population despite the fact that wide binaries are very sensitive to perturbation, a contact binary in a such compact configuration will keep its binarity (Parker et al. 2011).

Interestingly, based on our survey of cold classical light curves, we are not finding a lot of contact binaries in this population, which was the case in the Plutino one (Thirouin & Sheppard 2018, 2019). Assuming that escaped cold classicals classified as contact binaries were formed in their main reservoir, we should find a lot of contact binaries in the cold classical population. Therefore, it seems more likely that the escaped cold classical contact binaries were formed after or during their escape from the main reservoir. The different dynamical evolutions of the resonant TNOs compared to the cold classical population may help us understand how contact binaries form.

5. Summary and Conclusions

We report new color measurements for seven likely and potential contact binaries in the Kuiper Belt. Our results are as follows:

1. All the potential and likely contact binaries in the dynamically cold classicals display very red/ultra-red surface colors. These colors are typical for this subpopulation, thus they likely formed in situ.
2. The resonant TNOs reported in this work display a variety of colors, from moderately red to ultra-red. Four are very red and one is ultra-red, making them potentially escaped cold classicals. Four have moderately red surfaces and thus are not linked to the dynamically cold classical population. As moderately red surface colors are common in several sub-populations of TNOs, we cannot pinpoint their origins, but they were likely scattered to their current location.
3. There is a strong anti-correlation between inclination and g'–r'. A similar trend is noticed for the entire Kuiper Belt. We also present a potential correlation between perihelion distance and color, between rotational period and colors as well as an anti-correlation between eccentricity and color. It is unclear if these trends are real or are due our limited sample. Finding more contact binaries will help confirm these trends.
4. The escaped cold classicals classified as likely contact binaries can form in the main reservoir of the cold classical region or form once they are trapped in resonances. It is possible that resolved wide binaries escaped their main reservoir and through dynamical processes they shrunk their orbit and are now an end-state binary system in a contact configuration. A second option is that contact binaries were formed in the dynamically cold classical population and escaped as contact binaries. Because we are not finding a lot of contact binaries in the cold classical population, and because so far the resonances have been the most prolific, we suggest that the formation of contact binaries happened from dynamical interactions during or after their escape from the main reservoir.

We thank the referee for their careful reading of this paper and their comments. This paper includes data gathered with the 6.5 m *Magellan-Baade* Telescope located at las Campanas Observatory, Chile. We acknowledge the *Magellan* staff, and also acknowledge support from the National Science Foundation (NSF), grant No. AST-1734484 awarded to the "Comprehensive Study of the Most Pristine Objects Known in the Outer solar system."

ORCID iDs

Audrey Thirouin https://orcid.org/0000-0002-1506-4248
Scott S. Sheppard https://orcid.org/0000-0003-3145-8682

References

Agarwal, J., Jewitt, D., Mutchler, M., Weaver, H., & Larson, S. 2017, Natur, 549, 357
Batygin, K., Brown, M. E., & Fraser, W. C. 2011, ApJ, 738, 13
Benecchi, S., Borncamp, D., Parker, A., et al. 2018, Icar, in press
Benner, L. A. M., Busch, M. W., Giorgini, J. D., Taylor, P. A., & Margot, J.-L. 2015, in Asteroids IV, ed. P. Michel, F. E. DeMeo, & W. F. Bottke (Tucson, AZ: Univ. Arizona Press), 165
Boehnhardt, H., Delsanti, A., Barucci, A., et al. 2002, A&A, 395, 297
Brown, M. E., Barkume, K. M., Ragozzine, D., & Schaller, E. L. 2007, Natur, 446, 294
Campo Bagatin, A., Benavidez, P. G., Ortiz, J. L., & Gil-Hutton, R. 2016, MNRAS, 461, 2060
Carry, B., Snodgrass, C., Lacerda, P., Hainaut, O., & Dumas, C. 2012, A&A, 544, A137
Doressoundiram, A., Boehnhardt, H., Tegler, S. C., & Trujillo, C. 2008, in The Solar System Beyond Neptune, ed. M. A. Barucci et al. (Tucson, AZ: Univ. Arizona Press), 91
Doressoundiram, A., Peixinho, N., Moullet, A., et al. 2007, AJ, 134, 2186
Dotto, E., Perna, D., Barucci, M. A., et al. 2008, A&A, 490, 829
Fraser, W. C., & Brown, M. E. 2012, ApJ, 749, 33
Goldreich, P., Lithwick, Y., & Sari, R. 2002, Natur, 420, 643
Grundy, W. M., Benecchi, S. D., Porter, S. B., & Noll, K. S. 2014, Icar, 237, 1
Hastings, D. M., Ragozzine, D., Fabrycky, D. C., et al. 2016, AJ, 152, 195
Howell, S. B. 1989, PASP, 101, 616
Lacerda, P. 2011, AJ, 142, 90
Lacerda, P., & Jewitt, D. C. 2007, AJ, 133, 1393
Lacerda, P., McNeill, A., & Peixinho, N. 2014, MNRAS, 437, 3824
Leinhardt, Z. M., Marcus, R. A., & Stewart, S. T. 2010, ApJ, 714, 1789
Mann, R. K., Jewitt, D., & Lacerda, P. 2007, AJ, 134, 1133
Marsset, M., Fraser, W. C., Pike, R. E., et al. 2019, AJ, 157, 94
Massironi, M., Simioni, E., Marzari, F., et al. 2015, Natur, 526, 402
Moore, J. M., McKinnon, W. B., Cruikshank, D. P., et al. 2018, GeoRL, 45, 8111
Nesvorný, D. 2015, AJ, 150, 73
Nesvorný, D., & Vokrouhlický, D. 2019, Icar, 331, 49
Nesvorný, D., Youdin, A. N., & Richardson, D. C. 2010, AJ, 140, 785
Ortiz, J. L., Thirouin, A., Campo Bagatin, A., et al. 2012, MNRAS, 419, 2315
Parker, A. H., Kavelaars, J. J., Petit, J.-M., et al. 2011, ApJ, 743, 1
Peixinho, N., Boehnhardt, H., Belskaya, I., et al. 2004, Icar, 170, 153
Peixinho, N., Delsanti, A., & Doressoundiram, A. 2015, A&A, 577, A35
Petit, J.-M., Kavelaars, J. J., Gladman, B. J., et al. 2011, AJ, 142, 131
Pike, R. E., Fraser, W. C., Schwamb, M. E., et al. 2017, AJ, 154, 101
Porter, S. B., & Grundy, W. M. 2012, Icar, 220, 947

Rabinowitz, D. L., Benecchi, S., Grundy, W. M., Thirouin, A., & Verbiscer, A. J. 2017, AAS/DPS Meeting Abstracts, 49, 216.06
Rabinowitz, D. L., Benecchi, S., Grundy, W. M., Thirouin, A., & Verbiscer, A. J. 2018, Talk at the Transneptunian Solar System Conf., http://www2.mps.mpg.de/services/coimbra/
Ragozzine, D., & Brown, M. E. 2007, AJ, 134, 2160
Ryan, E. L., Sharkey, B. N. L., & Woodward, C. E. 2017, AJ, 153, 116
Schaller, E. L., & Brown, M. E. 2008, ApJL, 684, L107
Schlichting, H. E., & Sari, R. 2009, ApJ, 700, 1242
Schwamb, M. E., Fraser, W. C., Bannister, M. T., et al. 2018, arXiv:1809.08501
Sheppard, S. S. 2012, AJ, 144, 169
Sheppard, S. S., & Jewitt, D. 2004, AJ, 127, 3023
Sheppard, S. S., & Jewitt, D. C. 2002, AJ, 124, 1757
Sheppard, S. S., Ragozzine, D., & Trujillo, C. 2012, AJ, 143, 58
Smith, J. A., Allam, S. S., Tucker, D. L., et al. 2005, BAAS, 37, 131.11
Smith, J. A., Tucker, D. L., Kent, S., et al. 2002, AJ, 123, 2121
Snodgrass, C., Carry, B., Dumas, C., & Hainaut, O. 2010, A&A, 511, A72
Spearman, C. 1904, Am. J. Psychol., 15, 72
Stern, S. A., Weaver, H. A., Spencer, J. R., et al. 2019, Sci, 364, aaw9771
Tegler, S. C., & Romanishin, W. 2000, Natur, 407, 979
Tegler, S. C., Romanishin, W., & Consolmagno, G. J., S. J. 2016, AJ, 152, 210
Thirouin, A., Ortiz, J. L., Campo Bagatin, A., et al. 2012, MNRAS, 424, 3156
Thirouin, A., & Sheppard, S. S. 2017, AJ, 154, 241
Thirouin, A., & Sheppard, S. S. 2018, AJ, 155, 248
Thirouin, A., & Sheppard, S. S. 2019, AJ, 157, 228
Thirouin, A., Sheppard, S. S., Noll, K. S., et al. 2016, AJ, 151, 148
Thirouin, A., Sheppard, S. S., & Noll, K. S. 2017, ApJ, 844, 135
Trujillo, C. A., & Brown, M. E. 2002, ApJL, 566, L125
Trujillo, C. A., Sheppard, S. S., & Schaller, E. L. 2011, ApJ, 730, 105
Volk, K., & Malhotra, R. 2012, Icar, 221, 106